HHS Public Access

Author manuscript

Nature. Author manuscript; available in PMC 2015 April 30.

Published in final edited form as:

Nature. 2014 October 30; 514(7524): 650–653. doi:10.1038/nature13671.

Transcriptional interference by antisense RNA is required for circadian clock function

Zhihong Xue[1], **Qiaohong Ye**[1], **Simon R Anson**[3], **Jichen Yang**[2], **Guanghua Xiao**[2], **David Kowbel**[4], **N. Louise Glass**[4], **Susan K. Crosthwaite**[3], and **Yi Liu**[1,†]

[1]Department of Physiology, The University of Texas Southwestern Medical Center, 5323 Harry Hines Blvd., Dallas, TX 75390, USA

[2]Department of Clinical Sciences, The University of Texas Southwestern Medical Center, 5323 Harry Hines Blvd., Dallas, TX 75390, USA

[3]Faculty of Life Sciences, University of Manchester, Manchester M13 9PT, UK

[4]Department of Plant and Microbial Biology, University of California, Berkeley, CA 94720, USA

Abstract

Eukaryotic circadian oscillators consist of negative feedback loops that generate endogenous rhythmicities[1]. Natural antisense RNAs are found in a wide range of eukaryotic organisms[2-5]. Nevertheless, the physiological importance and mode of action of most antisense RNAs is not clear[6-9]. *frequency* (*frq*) encodes a component of the *Neurospora* core circadian negative feedback loop which was thought to generate sustained rhythmicity[10]. Transcription of *qrf*, the long non-coding *frq* antisense RNA, is light induced, and its level oscillates in antiphase to *frq* sense RNA[3]. Here we show that *qrf* transcription is regulated by both light-dependent and -independent mechanisms. Light-dependent *qrf* transcription represses *frq* expression and regulates clock resetting. *qrf* expression in the dark, on the other hand, is required for circadian rhythmicity. *frq* transcription also inhibits *qrf* expression and surprisingly, drives the antiphasic rhythm of *qrf* transcripts. The mutual inhibition of *frq* and *qrf* transcription thus forms a double negative feedback loop that is interlocked with the core feedback loop. Genetic and mathematical modeling analyses indicate that such an arrangement is required for robust and sustained circadian rhythmicity. Moreover, our results suggest that antisense transcription inhibits sense expression by mediating chromatin modifications and premature transcription termination. Together, our results established antisense transcription as an essential feature in a circadian system and shed light on the importance and mechanism of antisense action.

†Corresponding author: Yi Liu, Department of Physiology, ND13.214A, University of Texas Southwestern Medical Center, 5323 Harry Hines Blvd., Dallas, TX 75390-9040, Tel.: 214-645-6033, Fax: 214-645-6049, Yi.Liu@UTsouthwestern.edu.

Contributions: Z.X., S.A., S.K.C. and Y.L. designed experiments. Z.X., S.A., J.Y. and D.K. performed experiments. Q.Y. provided technical support. Y.L., Z.X., S.A., N.L.G. and S.K.C. analyzed data. Y.L., Z.X., and S.K.C. wrote the paper.

Competing financial interests: The authors declare no competing financial interests.

The transcription factors WHITE COLLAR (WC) -1 and -2 form a complex that activates *frq* transcription in the dark (DD) and mediates light-induced *frq* transcription for light-resetting of the clock by binding to light-responsive elements (LREs) on the *frq* promoter[11-13]. 3′ RACE and RNA sequencing showed that *frq* and *qrf* transcripts almost completely overlap (Figure 1a and Extended Figure 1a). In the *wc* mutants, *frq* expression was nearly abolished but *qrf* transcript was observed at ∼25% of wild-type levels (Figure 1b), indicating that both WC-dependent and -independent mechanisms mediate *qrf* transcription. WC complex binds to the *qrf* promoter region[14]. *frq* constructs with point mutations in each of the five putative binding sites in the *qrf* promoter were individually introduced into a frq^{10} (*frq* and *qrf* null) strain[15]. Mutation of only one site, qLRE, dramatically reduced *qrf* level (Figure 1c and Extended Data Figure 1b-d). In the frq^{qLREmut} strain, the *qrf* level was comparable to that of the *wc* mutant. In a qLRE knock-in strain ($frq^{\text{KI(qLREmut)}}$, Extended Data Figure 1e), *qrf* levels were also much lower than in the control knock-in strain and WC binding at the *qrf* promoter was completely abolished (Figure 1c-d and Extended Data Figure 1f), indicating that qLRE is the only WC binding site in the *qrf* promoter.

Coinciding with low levels of *qrf* in the qLRE mutant, higher than wild-type levels of *frq* mRNA and FRQ protein were observed (Figure 1c and Extended Data Figure 1d, 1f, 1g). *frq* and *qrf* are rapidly light-induced in the wild-type (Figure 1e) but in the frq^{10},frq^{qLREmut} strain, whereas *qrf* induction was completely abolished (Figure 1f), light-induction of *frq* was significantly elevated when compared to the wild-type, indicating that light induction of *qrf* represses light-induced *frq*. Circadian conidiation rhythms of qLRE mutant strains in DD were near normal, however, a light pulse resulted in significantly greater phase-shifts in the qLRE mutants than the controls (Figure 1g and Extended Data Figure 1h). These results are consistent with a previous report[3] and indicate that *qrf* regulates light resetting of the clock by repressing light-induced *frq*.

Similar levels of *qrf* transcripts seen in the $frq^{KI(WT)}$ and $frq^{KI(qLRE\ mut)}$ strains at DD24 (Extended Data Figure 2a) indicate that qLRE does not regulate *qrf* expression in DD. In a strain (frq^{10};frq.aq) in which the promoter of *qrf* was replaced with the quinic acid (QA)-inducible *qa-2* promoter, *qrf* expression was abolished in the absence of QA (Figure 2a). On addition of QA, *qrf* was induced but *frq* levels were significantly reduced, further indicating repression of *frq* by *qrf*.

A number of observations indicate that *qrf* expression must be within a certain range to permit a functional clock. Without QA, the frq^{10};frq.aq strain showed arrhythmic conidiation after the first day (Figure 2b and Extended Data Figure 2b). Moreover, a luciferase reporter (*Pfrq-luc*)[16] in the frq^{10};frq.aq strain showed that the circadian luciferase activity seen in the control strain was abolished, indicating that *qrf* expression is required for clock function (Figure 2c and Extended Data Figure 2c, 2d). As QA concentration increased, circadian conidiation rhythms were gradually restored in the frq^{10};frq.aq strain and at 10^{-5} -10^{-4} M QA, the rhythms were similar to the control strain (Figure 2b and Extended Data Figure 2b). At higher QA concentrations, however, the amplitudes of the rhythms reduced (Figure 2b) or became arrhythmic (Extended Data Figure 2b). In addition, the phase of the rhythms was significantly delayed without QA (Extended Data Figure 2e), a defect that was

also rescued by *qrf* induction. Restoration of circadian rhythms of FRQ expression, FRQ phosphorylation profiles and *frq* mRNA oscillation by QA was also seen in the frq^{10};frq.aq strain (Extended Data Figure 2f-g).

qrf RNA oscillates in DD in the wild-type in antiphase to *frq* (Figure 3a)[3] but WC-2 does not bind to the *qrf* promoter in DD (Extended Data Figure 3a). Moreover, the qLRE mutation did not affect either *frq* or *qrf* levels in DD (Extended Data Figure 3b), indicating that the WC complex does not regulate *qrf* transcription in DD. Crucially, a luciferase reporter (P*qrf-luc)* driven by the *qrf* promoter showed that the *qrf* promoter activity is not rhythmic in a wild-type strain (Figure 3b and Extended Data Figure 3c-d).

Several results indicate that *frq* and *qrf* mutually inhibit each other. 1) In a frq^9 mutant, only truncated FRQ protein is made, resulting in high *frq* levels [15] but reduced *qrf* levels (Extended Data Figure 3e). 2) When the frq^{10},$frq^{qLREmut}$ strain was exposed to light, induction of *frq* resulted in decreased *qrf* (Figure 3c). 3) Low *frq* mRNA levels in the wcc^{DKO} mutant led to elevated *qrf* levels in DD (Figure 3d).

To further investigate the regulation bewteen *frq* and *qrf*, we created a luciferase reporter construct (Pmin-*luc*-P*frq*), in which the luciferase sense mRNA is driven by a constitutive promoter[17] and antisense luciferase mRNA is driven by the *frq* promoter (Figure 3e). Wild-type strains containing the P*frq*-*luc* or Pmin-*luc* (lacking antisense luciferase RNA) construct were used as controls. Luminescence in the Pmin-*luc* strain was arrhythmic but the Pmin-*luc*-P*frq* strain exhibited a robust circadian luminescence rhythm antiphase to that of the P*frq*-*luc* rhythm (Figure 3e and Extended Data Figure 4a-b). These results indicate that the antiphasic rhythm of *qrf* expression is driven by rhythmic *frq* transcription independent of RNA sequence. Therefore, *frq* and *qrf* transcription forms a double negative feedback loop that results in antiphasic rhythms of *frq* and *qrf* (Figure 3f).

Mathematical modeling (Extended Data Figure 4c)[18] demonstrated that without *qrf* the *Neurospora* circadian oscillator can only generate a low amplitude *frq* oscillation that damps out quickly (Figure 3g). When the double negative feedback loops were introduced into the model, both *frq* and *qrf* levels oscillated robustly with antiphasic rhythms. When *qrf* was over-expressed, the *frq* oscillation could not sustain. These results suggest that the previously known circadian feedback loops, although not sufficient to sustain a persisting rhythm, are the source of the rhythmicity that is amplified and sustained by the resonance of mutually inhibitory and antiphasic expression of *frq* and *qrf*.

How do *qrf* and *frq* inhibit each other? Light-induced *frq* transcription, *frq* and *qrf* levels and circadian rhythms were normal in RNAi mutants (Extended Data Figure 5a-d)[19]. Convergent transcription is also known to induce DNA methylation in the *frq* region[20,21] but deletion of genes required for DNA methylation also did not affect *frq* expression (Extended Data Figure 5e-f).

We introduced a *frq* construct (qrf) with the *frq* promoter deleted into the frq^{10} and frq^{10};$frq^{qLRE\ mut}$ strains at the *csr-1* locus (Extended Data Figure 6a). This transgene can express normal levels of *qrf* without detectable *frq* expression (Extended Data Figure 6b). In

the *frq*^{10};frq$^{qLRE\ mut}$;qrf strains, even though *qrf* expression was restored to normal levels, *frq* levels were not rescued (Extended Data Figure 6c-d), indicating that *qrf* regulates *frq in cis*.

WC binding to the *frq* promoter initiates WC-dependent *frq* transcription, but the qLRE mutation did not affect WC binding at the *frq* promoter (Extended Data Figure 6e-f). However, However, levels of *frq* pre-mRNA were significantly elevated in the qLRE mutants (Figure 4a and Extended Data Figure 6g). Moreover, *qrf* expression in the *frq*^{10};frq.aq strain did not affect *frq* RNA stability (Extended Data Figure 6h). These results suggest that *qrf* regulates *frq* after transcriptional initiation.

After transcriptional initiation, RNA polymerase II CTD is phosphorylated at serines 2 and 5 with Ser 5 and Ser 2 phosphorylation enriched near the 5′ and 3′ ends of transcribed regions, respectively[22]. Similar Ser 5 and Ser 2 phosphorylation profiles were seen at a *Neurospora* locus without antisense transcripts (Extended Data Figure 7a-b). In contrast, both modifications of CTD peaked at the same position in the middle of the transcribed *frq* region (Figure 4b, Extended Data Figure 8). Mutation of the qLRE, which reduces *qrf* expression, resulted in decreases of both Ser 2 and Ser 5 phosphorylation. Phosphorylation of pol II can trigger histone H3K36 methylation[23]. H3K36me3 enrichment at the *frq* locus peaked at the same position as did CTD phosphorylation, and the qLRE mutation reduced H3K36me3 (Figure 4b, bottom panel). In the *frq*^{10};frq.aq strain minus QA, in which *qrf* expression is completely abolished, the distributions of CTD phosphorylation and H3K36me3 on *frq* resemble the control locus lacking antisense transcription (Extended Data Figure 9a-c). These results suggest that pol II stalls in the middle of *frq* locus due to convergent transcription[9].

SET-2 methylates H3K36 in *Neurospora*[24] and is required for clock function[25]. Even though *frq* and *qrf* levels were only modestly increased in the *set-2*^{KO} single mutants, their levels were markedly elevated in the *frq*^{9}*;set-2*^{KO} double mutant (Figure 4c and Extended Data Figure 10a), suggesting that H3K36me3 contributes to the suppression of *frq* and *qrf* transcription. However, the induction of *qrf* still resulted in a reduction of *frq* in the *set-2*^{KO}*, frq*^{10} double mutant strain (Figure 4d and Extended Data Figure 10b), indicating the existence of another mechanism that mediates the action of antisense transcription.

Stalled pol II due to convergent transcription may abort transcription prematurely, which should result in truncated transcripts from their respective 5′ ends. We screened a panel of *Neurospora* mutants for the nuclease that degrades such transcripts. The RNA exosome is involved in degrading full-length *frq* transcripts[26]. Northern blot analysis using an RNA probe (*frq*-N term or *qrf*-N-term) specific for the 5′ end of *frq* or *qrf*, respectively, revealed that the silencing of *rrp44*, which encodes the exosome catalytic subunit, resulted in the appearance of a low molecular weight RNA smear in the wild-type strain (Figure 4e and Extended Data Figure 10c). In contrast, a probe specific for the 3′ half of *frq* failed to detect the RNA smear. Importantly, the amount of the RNA smear was dramatically decreased in the qLRE mutant (Figure 4f) and was not observed for a control gene without antisense transcripts (Extended Data Figure 10d). Together, these results suggest that both premature

transcription termination and chromatin modifications contribute to the transcriptional inhibition of *frq* by *qrf*.

We discovered here that sense and antisense transcription of *frq* forms a double negative feedback loop that is interlocked with the core circadian feedback loops in *Neurospora*. The mutual transcription interference of *frq* and *qrf* results in antiphasic oscillations of *frq* and *qrf* that resonate to achieve robust and sustained circadian gene expression. In the silkmoth and mouse liver, antisense *per* RNAs exist and were also found to oscillate in antiphase to sense RNAs [27-30], suggesting that a similar mechanism may also function in animal circadian systems.

Methods

Strains, plasmid constructs, and growth conditions

The wild-type strain used in this study was 87-3 (*ras-1bd*, a). The frq^{10} strain is a *frq*-null and *qrf*-null mutant [15]. The frq^{9} strain bears a frame-shift mutation in the *frq* ORF [15]. The mutants $wc\text{-}1^{RIP}$, $wc\text{-}2^{KO}$, wcc^{DKO} ($wc\text{-}1^{RIP}$, $wc\text{-}2^{KO}$), dcl^{DKO} ($dcl\text{-}1^{RIP}$, $dcl\text{-}2^{KO}$), $qde\text{-}1^{KO}$, $qde\text{-}2^{RIP}$, $qde\text{-}3^{KO}$ were generated in previous studies [12,31]. The $dim\text{-}2^{KO}$ and $dim\text{-}5^{KO}$ strains were generously provided by Dr. Qun He [32]. The $set\text{-}2^{KO}$ (FGSC #15505) strain was from Fungal Genetic Stock Center (FGSC). The $set\text{-}2^{KO}$;frq^{9} double mutant was created in this study by crossing $set\text{-}2^{KO}$ and frq^{9}. The *dsrrp44* strain was generated by introduction of a plasmid expressing quinic acid-driven *rrp44*-specific RNA hairpin into a wild-type strain [26]. The $frq^{KI(WT)}$ and $frq^{KI(qLRE\ mut)}$ strains were created in this study (Extended Data Figure 1b, 1e). The $frq^{KI(qLRE\ mut)}$; *dsrrp44* strain was created by crossing $frq^{KI(qLRE\ mut)}$ and *dsrrp44*. The frq^{10};frq^{WT}, frq^{10};$frq^{qLREmut}$, frq^{10};frq.aq strains were obtained by targeting plasmids pKAJ120, pKAJ120$^{qLRE\ mut}$, and pKAJ120.aq, respectively, into the *his-3* locus of the frq^{10} mutant as previously described [15] (Extended Data Figure 1c). The frq^{10};$frq^{qLRE\ mut}$;qrf strain was generated by targeting the plasmid pCSR1.qrf into *csr-1* locus of the frq^{10};$frq^{qLRE\ mut}$ mutant as previously described [33] (Extended Data Figure 6a).

The pKAJ120 that contains the entire wild-type *frq* gene including its promoter and a *his-3* targeting sequence was used as the parental plasmid [15]. The qLRE in pKAJ120 was mutated as described (Extended Data Figure 1b) by site-directed mutagenesis to create pKAJ120$^{qLRE\ mut}$. The fragment between *BssH*II and *Sap*I sites of pKAJ120 was replaced with an inverted *Neurospora qa-2* promoter to create pKAJ120.aq. The PCR fragment containing entire wild-type *qrf* and its promoter (primer: 5′-TTCATTAAGGTGGGGCAGG-3′, 5′-TTTCCACGCCGGCCCCAGTC-3′) was inserted into vector pCSR1 between *Not*I and *Pst*I sites to generate pCSR1.qrf [33].

Growth conditions were described previously [15]. Liquid cultures were grown in minimal medium (1×Vogel's, 2% glucose). When quinic acid (QA) was used, liquid cultures were grown in low glucose medium (1×Vogel's, 0.1% glucose, 0.17% arginine) with indicated concentrations of QA. For *rrp44* knockdown assay, *Neurospora* was cultured into mats in low glucose medium with 10^{-2} M QA for 2 days. Afterwards, *Neurospora* mats were cut into discs and cultured in flasks in same medium with shaking. After 2 days, the tissues were harvested. For the mRNA decay assay, the cultured conditions were described previously [26].

For rhythmic experiments, the *Neurospora* cultures were transferred from LL to DD at time 0 and were collected in DD at the indicated time (hours). For light induction, *Neurospora* cultures were grown in DD for 24 hrs with shaking, and then treated with 1750 lux light pulse. Afterwards, *Neurospora* cultures were transferred back to DD and collected at the indicated time (minutes). For race tube assay, the medium contains 1× Vogel's, 0.1% glucose, 0.17% arginine, 50 ng·ml^{-1} biotin, and 1.5% agar with indicated concentrations of QA (for data shown in Extended Data Figures 2b, glucose was not present in the medium). Strains were inoculated and grown in constant light at 25 degree for 24 hrs before being transferred to DD at 25 degree. Calculations of period length and phase were performed as described [34].

Analysis of phase response to light

The assay was performed on race tubes containing acetate/casamino acid medium (1× Vogel's, 1.2% sodium acetate, 0.05% casamino acid hydrolysate, and 1.5% agar) [35]. Race tubes were first grown in LL at 25 degree for 48 hrs before being transferred to DD. Cultures were then grown in DD at 25 degree for 25 hrs, and different individual cultures were given a 2-min light pulse (1750 lux) at different times (2 hrs intervals) to cover an entire circadian cycle. The amount of phase shift was determined by comparing light-treated cultures (6 replicas for each time point) with those of the control cultures (kept in DD). The initial LL to DD transition was defined as circadian time (CT) 12. The phases of the cultures were calculated as the average phase for 2 consecutive days after the light treatment.

Protein and RNA analysis

Tissue harvest, protein extraction, and western blots were performed as previously described [15]. For protein separation, 40 μg total protein loaded in each lane of SDS-PAGE (7.5%). Total RNA was extracted with Trizol in accordance with the manufacturer's protocol, and then further purified by 2.5M LiCl as previously described [36]. Northern blot analyses were performed as previously described using [^{32}P]UTP-labeled riboprobes [15]. Riboprobes were transcribed *in vitro* from PCR products by T3 or T7 RNA polymerase (Ambion) with the manufacturer's protocol. The primer sequences used for the template amplification were *frq*-N term (5′- TAATACGACTCACTATAGGG (T7 promoter) GGCAGGGTTACGATTGGATT-3′, 5′-GGGTAGTCGTGTACTTTGTCAG-3′), *frq*-C term (5′-TAATACGACTCACTATAGGG (T7 promoter) CCTTCGTTGGATATCCATCATG-3′, 5′- GAATTCTTGCAGGGAAGCCGG-3′), *qrf*-N term (5′-AATTAACCCTCACTAAAGGG (T3 promoter) GAATTCTTGCAGGGAAGCCGG-3′, 5′- CCTTCGTTGGATATCCATCATG-3′), and NCU01953 N-term (5′ TAATACGACTCACTATAGGG (T7 promoter) GTGCCAAAGAGTTGGCCATTC-3′, 5′- CTTGCACCACAAACTGTTGAAC-3′). Except for results shown in Figure 4e-f, riboprobes of *frq*-C term and *qrf*-N term were used for detecting *frq* and *qrf*, respectively. For Figure 4e-f and Extended Data Figure 10, the riboprobes were hydrolyzed for 25 mins in 40 mM Na_2CO_3, 60 mM $NaHCO_3$, 10 mM 2-mercaptoethanol, and then the reaction was stopped with an equal volume of 0.2 M NaOAC, pH 6.0, 1% HOAC, 10 mM DTT. For western blot and northern blot, densitometry analyses were performed using Image J.

Quantitative PCR (qPCR) and quantitative reverse transcriptase PCR (RT-qPCR) were performed as previously described [26]. For strand-specific RT-qPCR, several modifications of the protocol were made. The primer sequences for strand-specific RT reactions were *frq* (5′-GCTAGCTTCAGCTAGGCATC (adaptor) CGTTGCCTCCAACTCACGTTTCTT-3′), *qrf* (5′-CCTCAGCTCGTACGAGTCGTAC (adaptor) GTCATGGAGCCCTCTGGTCTTGGT-3′), *frq* pre-mRNA (5′-GCTAGCTTCAGCTAGGCATC (adaptor) TTGAACGGTAGGGAGGAGGAGAG-3′), and *β-tubulin* (5′-CTCGTTGTCAATGCAGAAGGTC-3′). The RT reaction was performed by mixing the primers of specific strand and *β-tubulin. β-tubulin* was used for internal control. The primer sequences for the qPCR step of RT-qPCR assay were *frq* (5′-AGCTTCAGCTAGGCATCCGTT-3′, 5;- GCAGTTTGGTTCCGACGTGATG-3′), *qrf* (5′-CAGCTCGTACGAGTCGTACGTC-3′, 5′- ATCTTCCGATGTTGTCGAGCGT-3′), *frq* pre-mRNA (5′- AGCTTCAGCTAGGCATCTTGAACG-3′, 5′-ACGGCATCTCATCCATTCTCACCA-3′), and *β-tubulin* (5′-ATAACTTCGTCTTCGGCCAG-3′, 5′- ACATCGAGAACCTGGTCAAC-3′).

Strand-specific RNA Seq

Approximately 10^6 /ml conidia were inoculated into 30 ml of VMM with 2% sucrose and incubated at 25°C for 20 hrs with shaking. The mycelia was filtered through Whatman paper and washed once with ice cold phosphate buffered saline. Approximately 200 mg was put into a 2.0 ml cryo vial with silicon beads and frozen in liquid nitrogen. Total RNA was isolated from frozen mycelia in 1.0 ml TRIzol using a BioSpec beater. Five μg total RNA was run out on a 1.0% agarose gel to check for degradation. The 3′ paired-end RNAseq library was prepared from 10 μg total RNA as described [37]. Briefly, the poly(A)$^+$ fraction was isolated on oligo(dT)$_{25}$ magnetic beads [Invitrogen] then treated to chemical fractionation with ZnCl (Ambion) followed by another round of poly(A)$^+$ enrichment. First strand cDNA was generated from an anchored oligo(dT)$_{20}$ primer followed by second strand synthesis with DNA polymerase I. The addition of paired-end adaptors and size isolation with ampureXP beads (Ambion) was followed by PCR enrichment are described [37]. The library has an average insert size of 200 bp ± 36 bp. The library was sequenced to a depth of 22 million 36 bp paired-end reads on an Illumina GAIIx sequencer. The access number is SRP030415.

Nascent nuclear transcripts isolation

Liquid cultures were grown in 1L minimal medium (1×Vogel's, 2% glucose). The dried frozen tissue (∼4g) was ground in liquid N_2. 8 ml of cold Buffer A (1M Sorbitol, 7% ficol, 20% glycerol, 5mM Mg(Ac)$_2$, 3mM $CaCl_2$, 50mM Tris.Cl pH7.5, 3mM DTT, 10μg/ml leupeptin, 10μg/ml pepstatin, 10μg/ml PMSF) was mixed with tissue powder on ice for 5-10min with stirring. The mixture was filtered through 4 layers pre-wet miracloth (Buffer A) into small flask on ice. Buffer A was added into filtered mixture till the volume is up to 8 ml. 16ml pre-chilled Buffer B (10% glycerol, 5mM Mg(Ac)2, 25mM Tris.Cl pH7.5, 10μg/ml leupeptin, 10μg/ml pepstatin, 10μg/ml PMSF) was slowly added with stirring. The obtained mixture was gently laid onto 10 ml of pre-chilled buffer A/B (2.5:4) in 50 ml of screw-cap tube. The supernatant was collected after centrifuging at 3000g for 7min at 4 degree. 33ml of the supernatant was gently laid onto 5 ml of pre-chilled Buffer D (1M

Sucrose, 10% glycerol, 5mM $Mg(Ac)_2$, 25mM Tris.Cl pH7.5, 1mM DTT, 10μg/ml leupeptin, 10μg/ml pepstatin, 10μg/ml PMSF). The pellet (purified nuclei) was collected after centrifuging at 9400g for 15min at 4 degree. The pellet was suspended by 1ml Trizol. Total RNA was extracted with Trizol in accordance with the manufacturer's protocol. The contaminated DNA was removed using TURBO DNA-free™ Kit following the manufacturer's protocol. 50ng of treated RNA was used for strand-specific RT-qPCR.

Chromatin immunoprecipitation (ChIP) assay

The ChIP assay was performed as previously described with several modifications [38]. First, 500 μg total cell lysis was used for each immunoprecipitation assay. The antibodies used in this study were WC-2 [12](2 μl/assay), Pol II CTD (Abcam #ab26721, 2μg/assay), Pol II S2P-CTD (Abcam #ab5095, 2 μg/assay), Pol II S5P-CTD (Abcam #ab5131, 2 μg/assay), Histone H3 (Abcam #ab1791, 2μg/assay) and H3K36me3 (Abcam #ab9050, 2 μg/assay). Each experiment was independently performed three times, and immuoprecipitation with IgG or wcc^{DKO} extract was used as the negative control. qPCR was used for measuring the immunoprecipitated DNA. Primer sequences for qPCR were *frq* dLRE (5′-AGAGTTTGGCCGGACAACCAGTA-3′, 5′-GCTTCGACCGAAAGTATCTTGAGCCT-3′), *frq* pLRE (5′-GTCGCAGAGGACCCTGAACTTT-3′, 5′-TCCCACAGATGCACAGGAATCG-3′), and *qrf* qLRE (5′-ATCGATCACTAGTCCCGGTTCGTT-3′, 5′-TTGCTGATAATGCGCTGAGGGTCT-3′). For experiments in Figure 4b and Extended Data Figure 8 and 9, the primer sequences were 1 (5′-AGAGTTTGGCCGGACAACCAGTA-3′, 5′-GCTTCGACCGAAAGTATCTTGAGCCT-3′), 2 (5′-GGGTAGTCGTGTACTTTGTCAG-3′, 5′-ACCGGACTTTAGGTTGTGTG-3′), 3 (5′-ACGGCCTTTCTCTGTTTACC-3′, 5′-GCAGAGTTGGGTCGGATTTA-3′), 4 (5′-CCGTTCTAGCGTGCTTCTT-3′, 5′-GGCACTAATGAGGTTCGAGATT-3′), 5 (5′-TTACTTCATCTTCCGCACTGG-3′, 5′-GGCAGGGTTACGATTGGATT-3′), 6 (5′-ACTGTTCACCGGAAAGATCAG-3′, 5′-GGGCCATGTTGGTTCCTT-3′) 7 (5′-TTGCACCGATCTTTCAGGAG-3′, 5′-CTGCAGCACATGTTCAACTTC-3′), 8 (5′-GGGCAGAGAGTGGCTATAGTA-3′, 5′-CCGCGTCTTCTTCTCACATAG-3′). For experiments in Extended Data Figure 7, the primer sequences were 1 (5′-CAAGTGGGCCCTACAGTTATT-3′, 5′- CCAATCCACTTCCCTTTCCA-3′), 2 (5′-CACCGTGTTCGTGCTTACT-3′, 5′- GGTATCCGTCTTGTCCCTTTG-3′), 3 (5′-TCAAGATACGGAGCGAAGAATG-3′, 5′- GATTGTAGCTGTTCCACCTCTC-3′), 4 (5′-TGACCGACCCAGTTGATTTC-3′, 5′- GTGGCACTTCTATCACCTTCTT-3′), 5 (5′-CGACCGTTAGGAGACCAAATAG-3′, 5′-AATGGCTTCCTTGTGGTTAGA-3′), 6 (5′-CTTAGTCGGATCAGTGGCTATT-3′, 5′- TTCGTAGATGCCGTGAGATG-3′), 7 (5′-CGTGGACTTCTGCTACTCTTC-3′, 5′- CCTTTGCAGTCCTCCTCTTT-3′), 8 (5′-GTCTGGGAGCTTCTGTTGAATA-3′, 5′- TAAAGTGGTGAACGACCTCATC-3′).

Luciferase reporter assay

The luciferase reporter assay was performed as previously described [16]. The reporter construct in Figure 2c (P*frq-luc*) was generated by inserting *BamH*I-*Not*I fragment of P*frq-luc*-I (a generous gift from J. Dunlap) into corresponding sites of pBARKS1 [16]. The reporter

construct in Figure 3b (P*qrf-luc*) was generated by inserting the PCR fragment containing *qrf* promoter and luciferase gene into *Not*I-*Eco*RI sites of pBARKS1. For the PCR fragment, *qrf* promoter was directly fused with luciferase gene ORF. The primer sequences were *qrf* promoter (5′-ATCGATTTCATTAAGGTGGGG-3′, 5′-GGTGGTGGGTGGTGGGTGGAG), and luciferase gene (5′-ATGGAGGACGCCAAGAACATCAAG-3′, 5′- TCAGAGCTTGGACTTGCCGCC-3′). The plasmids P*frq-luc* and P*qrf-luc* were transformed into wild-type or frq^{10};frq.aq strains with Ignite selection as previously described [39]. The plasmid P*min.luc* was generated by inserting the luciferase gene ORF into *Xma*I site of pDE3dBH. The plasmid P*min.luc*.P*frq* was generated by inserting inverted *frq* promoter (the same as P*frq-luc*-I) into downstream of luciferase gene ORF of P*min.luc*. The non-regulated basal promoter in pDE3dBH (upstream of *Eco*RI site) was used as the minimal promoter to control the expression of luciferase gene in *Pmin.luc* and P*min.luc*.P*frq* as previously described [17]. For Figure 3e, the plasmids P*frq-luc*-I, P*min.luc*.P*frq*, and P*min.luc* were transformed into the wild-type strain by targeting *his-3* locus. Under our experimental condition, luciferasae signals are highly variable during the first 1-2 days in the LumiCycle and only become stabilized afterwards, which is likely due to an artifact caused by the light-dark transfer of the cultures. Thus, the results presented were recorded after 1-2 days in DD.

Mathematical modeling

The mathematical simulation of relative *frq* and *qrf* RNA levels in DD was performed based on a previously described model [18,40-42] with several modifications. The equations used here are listed in Extended Data Figure 4c.

The differential equations (1) through (8) were solved numerically by the Gear method and XPPAUT [43,44]. The parameters were as follows: The values of k_2, k_3, k_6, k_7, k_8, k_9, k_{11}, k_{12}, k_{13}, k_{14}, k_{15}, K, K_2, k_{01} were from a previous study [18]. The values of k_4 and k_5 were from previous study [40,41]. The value of k_{10} was from a previous study [42]. The values of other parameters were determined in this study. For Figure 3g, $k_{19} = 0$ (left panel); $k_{17} = 0.35$, $k_{19} = 0.1$ (middle panel); $k_{19} = 0.1$, $k_{17} = 0.35$, $k_{16} = 0.91$ (right panel).

Extended Data

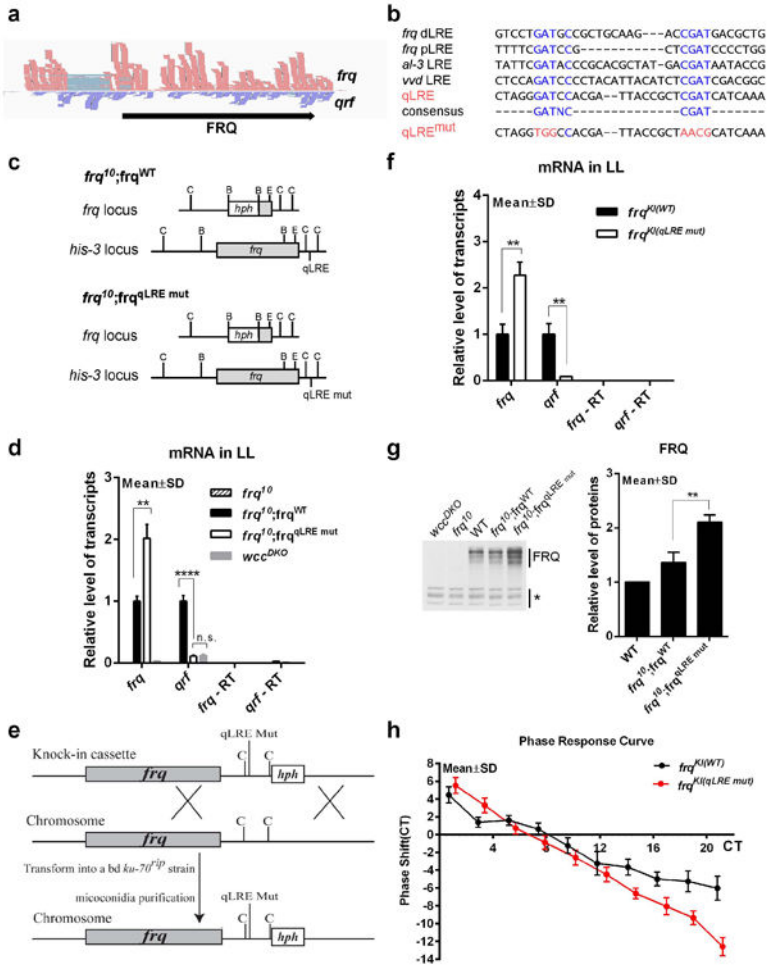

Extended Data Figure 1.

Light-induced *qrf* expression represses *frq* transcription and regulates light resetting of the clock. (a) Strand-specific RNA-Seq result of the *frq* locus showing the overlapping *frq* and *qrf* transcripts. (b) Sequence alignment of known LRE elements. The qLRE and the mutated regions in the *qrf* promoter are shown. (c) Diagrams showing the chromosomal modifications in the indicated loci in the frq^{10};frq^{WT} and frq^{10};$frq^{qLRE\ mut}$ strains. C, *Cla* I; B, *Bgl* II; E, *Eco*R V. (d) Strand-specific RT-qPCR results showing the expression levels of *frq* and *qrf* in indicated strains in LL. Error bars are standard deviations (n=3). Asterisks indicate P value < 0.01. n.s. indicates that the difference is not statistically significant. *frq*-RT and *qrf* –RT represent the non-RT reaction control. (e) Diagram describes the strategy used to obtain the knock-in strains by homologous recombination. (f) Strand-specific RT-qPCR results showing the expression levels of *frq* and *qrf* in the indicated knock-in strains in LL. (g) Western blot results showing the FRQ expression levels in the indicated strains in LL. The densitometric analysis of western blot results from three independent experiments is shown at right. Error bars are standard deviations. Asterisks indicate P value < 0.01. (h) Phase response curves of circadian conidiation rhythms of the indicated knock-in strains after 2 min of light pulse at different circadian time (CT) points.

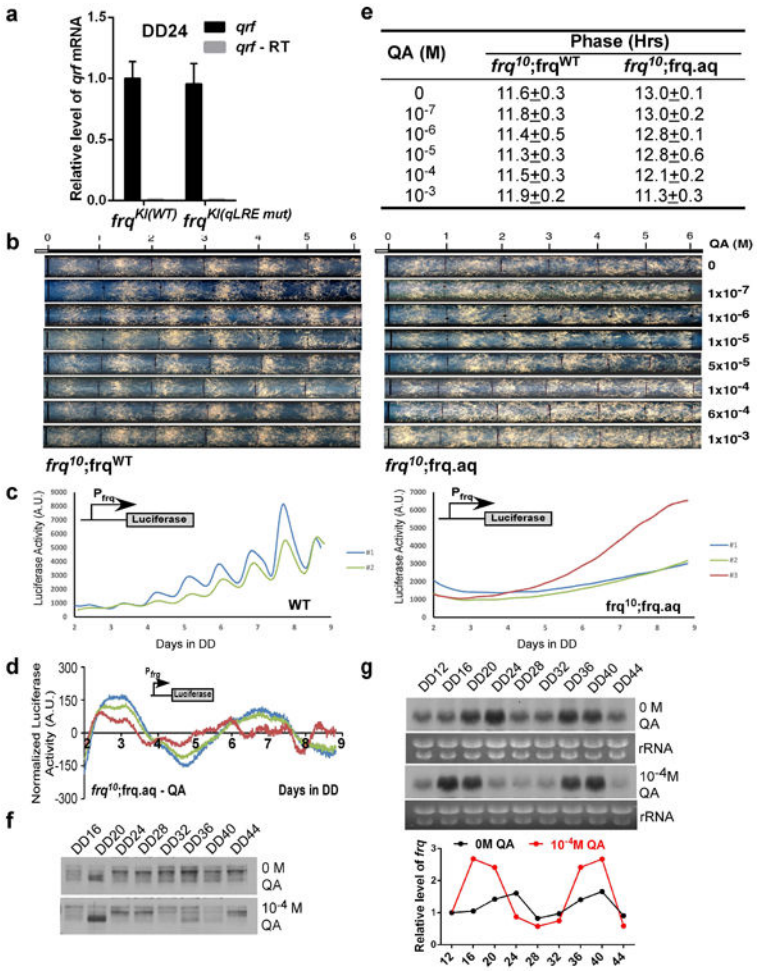

Extended Data Figure 2.

qrf expression is required for circadian rhythmicities. (a) Strand-specific RT-qPCR results showing the expression levels of *qrf* in the indicated knock-in strains at DD24. (b) Race tube analyses of the *frq*^{10};frq^{WT} and *frq*^{10};frq.aq strains in medium containing 0% glucose, 0.17% arginine with the indicated concentrations of QA in DD. The lack of glucose in medium is known to allow more efficient expression from the *qa-2* promoter. The black lines on race tubes indicate the daily growth fronts. (c) The unnormalized luciferase activity of the experiments in Figure 2c. (d) The normalized result of Figure 2c in 10× scale showing fluctuation of the luciferase activity in the *frq*^{10};frq.aq strain is random and not rhythmic in the *frq*^{10};frq.aq strain. (e) A table showing the phases of the first conidiation band in DD of the race tube results shown in Figure 2b. (f) Western blot analysis showing the FRQ expression profiles in the *frq*^{10};frq.aq strain with/without QA in DD at the indicated time points. (g) Northern blot analysis showing *frq* expression profiles in the *frq*^{10};frq.aq strain in DD at the indicated time points. The densitometric analysis is shown below.

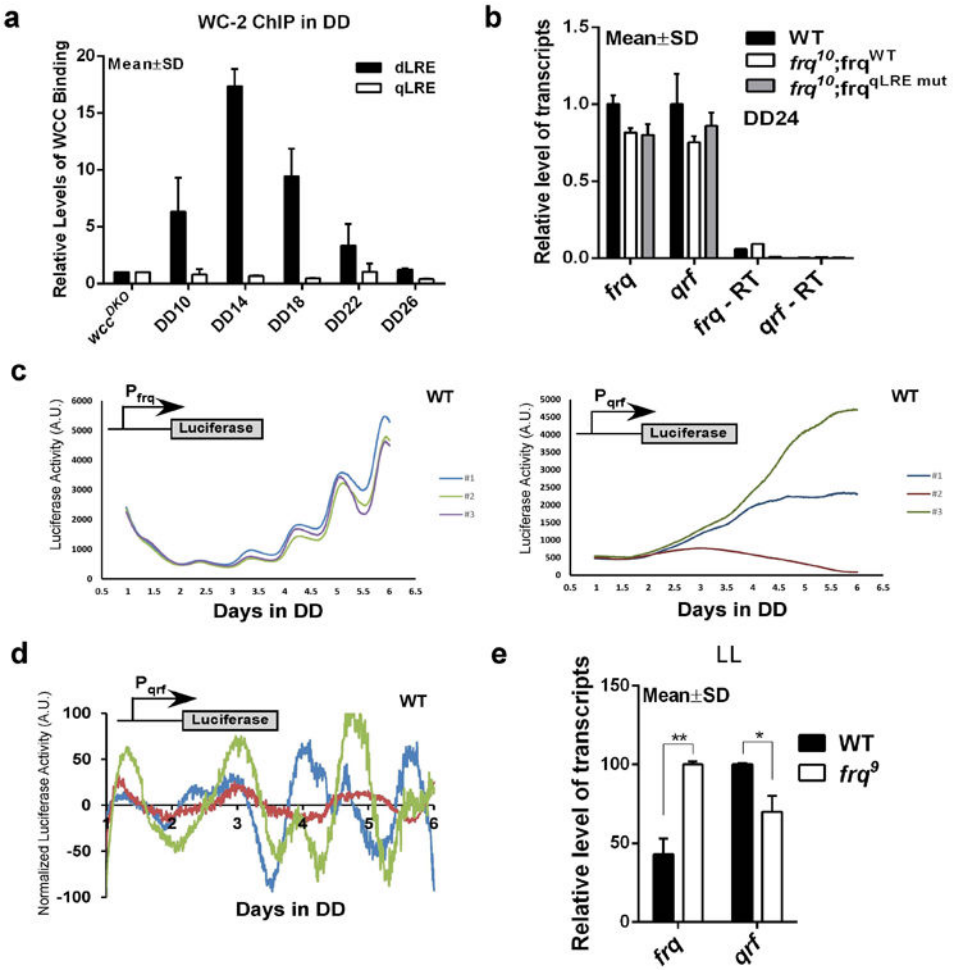

Extended Data Figure 3.

(a) WC complex does not bind to the *qrf* promoter in DD. WC-2 ChIP assays showing the relative levels of WC binding at the *frq* (dLRE) and *qrf* (qLRE) promoters at the indicated time points in DD. (b) Strand-specific RT-qPCR results showing the levels of *frq* and *qrf* at DD24 in the indicated strains. (c) The unnormalized luciferase activity of the experiments in Figure 3b. (d) The normalized luciferase activity of the Pqrf:luc construct in Figure 3b shown in 10× scale (e) Densitometric analyses of three independent northern blot results indicate that levels of *qrf* transcripts are reduced in the *frq*^{9} strains as a result of increased *frq* expression.

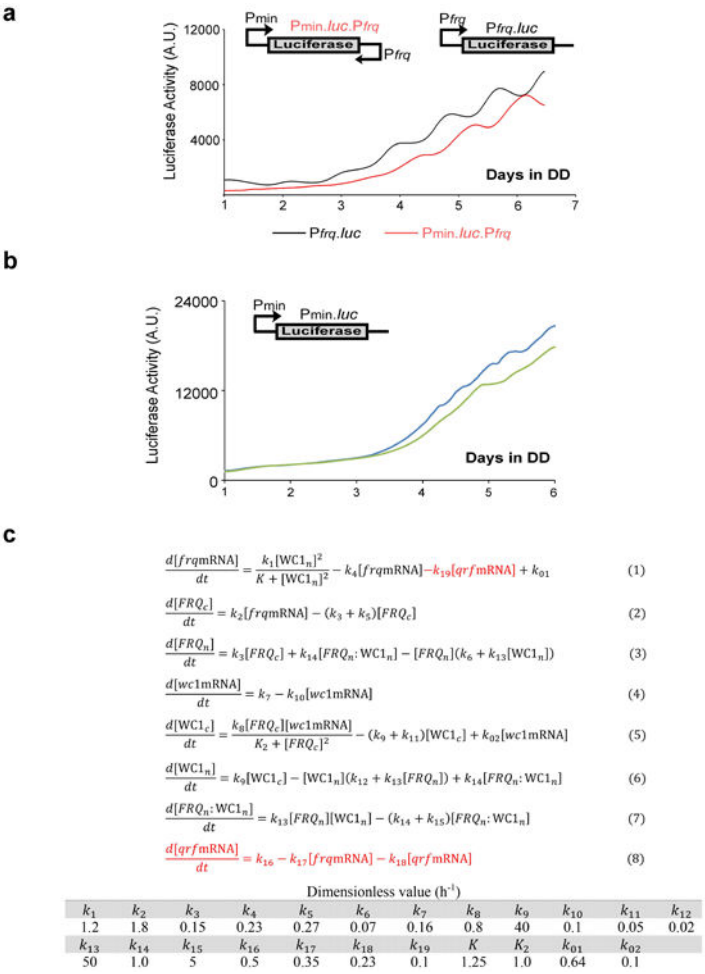

$$\frac{d[frq\text{mRNA}]}{dt} = \frac{k_1[\text{WC1}_n]^2}{K + [\text{WC1}_n]^2} - k_4[frq\text{mRNA}] - k_{19}[qrf\text{mRNA}] + k_{01} \quad (1)$$

$$\frac{d[FRQ_c]}{dt} = k_2[frq\text{mRNA}] - (k_3 + k_5)[FRQ_c] \quad (2)$$

$$\frac{d[FRQ_n]}{dt} = k_3[FRQ_c] + k_{14}[FRQ_n{:}\text{WC1}_n] - [FRQ_n](k_6 + k_{13}[\text{WC1}_n]) \quad (3)$$

$$\frac{d[wc1\text{mRNA}]}{dt} = k_7 - k_{10}[wc1\text{mRNA}] \quad (4)$$

$$\frac{d[\text{WC1}_c]}{dt} = \frac{k_8[FRQ_c][wc1\text{mRNA}]}{K_2 + [FRQ_c]^2} - (k_9 + k_{11})[\text{WC1}_c] + k_{02}[wc1\text{mRNA}] \quad (5)$$

$$\frac{d[\text{WC1}_n]}{dt} = k_9[\text{WC1}_c] - [\text{WC1}_n](k_{12} + k_{13}[FRQ_n]) + k_{14}[FRQ_n{:}\text{WC1}_n] \quad (6)$$

$$\frac{d[FRQ_n{:}\text{WC1}_n]}{dt} = k_{13}[FRQ_n][\text{WC1}_n] - (k_{14} + k_{15})[FRQ_n{:}\text{WC1}_n] \quad (7)$$

$$\frac{d[qrf\text{mRNA}]}{dt} = k_{16} - k_{17}[frq\text{mRNA}] - k_{18}[qrf\text{mRNA}] \quad (8)$$

Dimensionless value (h^{-1})

k_1	k_2	k_3	k_4	k_5	k_6	k_7	k_8	k_9	k_{10}	k_{11}	k_{12}
1.2	1.8	0.15	0.23	0.27	0.07	0.16	0.8	40	0.1	0.05	0.02
k_{13}	k_{14}	k_{15}	k_{16}	k_{17}	k_{18}	k_{19}	K	K_2	k_{01}	k_{02}	
50	1.0	5	0.5	0.35	0.23	0.1	1.25	1.0	0.64	0.1	

Extended Data Figure 4.

(a) The unnormalized luciferase activity of the experiments in Figure 3e. (b) The unnormalized luciferase activity of the wild-type strain carrying the Pmin-*luc* construct. Results of two independent transformants were shown. (c) Mathematical modeling of the *Neurospora* circadian oscillator with the double negative feedback loop. The differential equations used in the model are shown. The model is identical to a previously developed model[23] with the exception of equation 1, which in this case includes the inhibition of *frq* transcription by *qrf*, and the equation 8, which includes the inhibition of *qrf* transcription by *frq*. The rate constants used in the simulations were listed below.

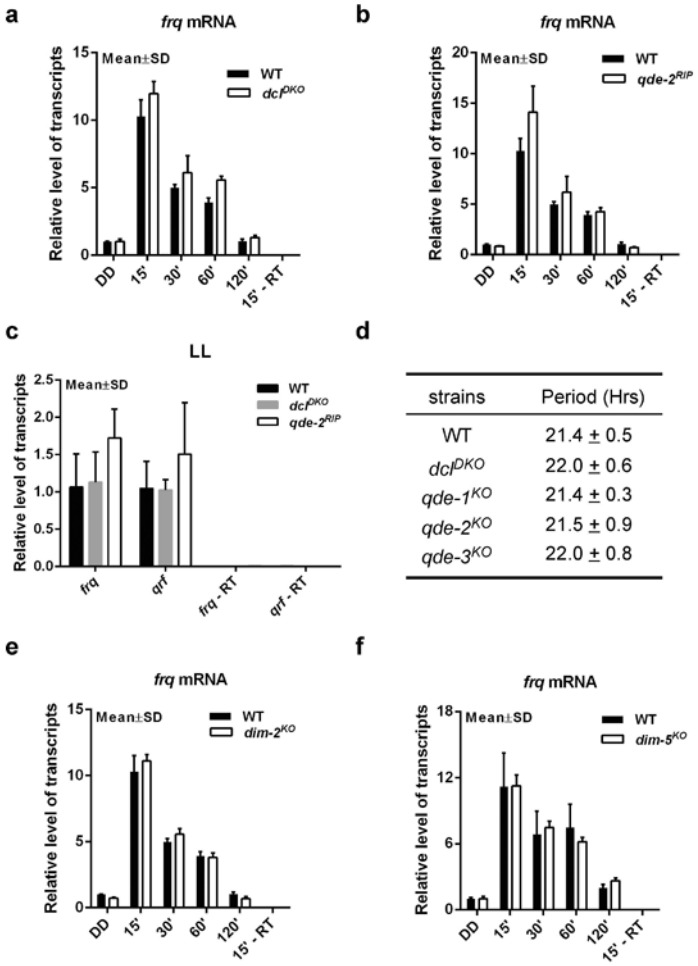

Extended Data Figure 5.

Neither RNAi nor DNA methylation pathways play a significant role in the clock. (a-b) Strand-specific RT-qPCR results showing the induction of *frq* after a light pulse are similar in the indicated trains at DD24. (c) Strand-specific RT-qPCR results showing similar expression levels of *frq* and *qrf* in the indicated strains in LL. (d) A table showing the period lengths of the conidiation rhythms in the wild-type and different RNAi mutants. (e-f) Strand-specific RT-qPCR results showing the induction of *frq* after a light pulse is similar in the indicated trains at DD24. Error bars are standard deviations (n=3).

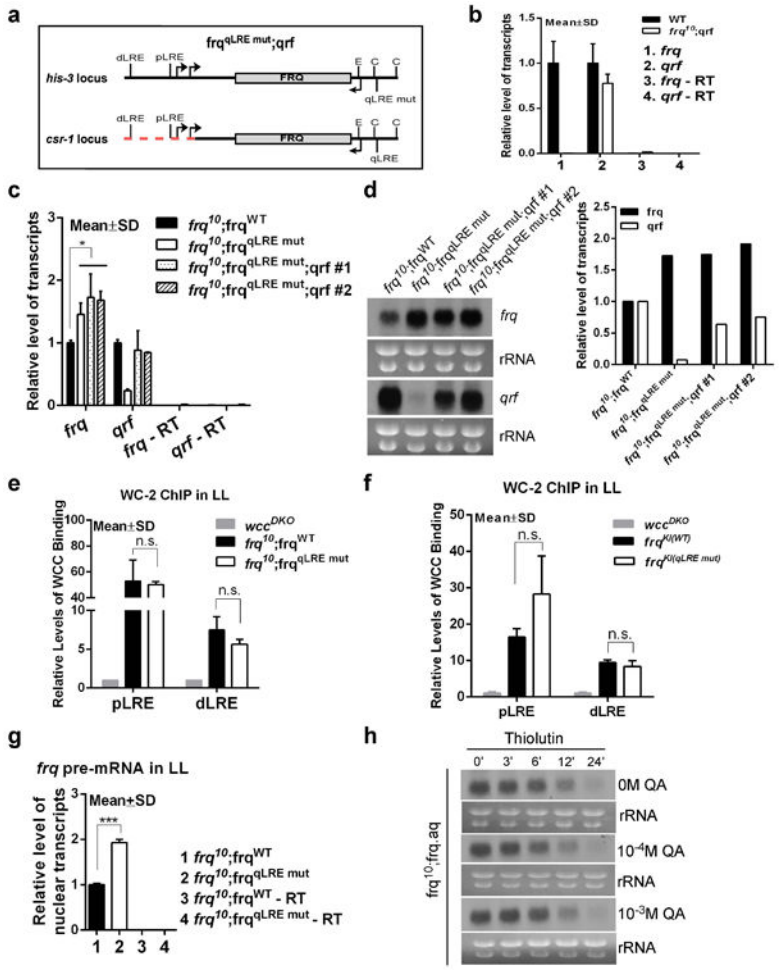

Extended Data Figure 6.

(a) A diagram showing the chromosomal modifications in the *frq*$^{qLRE\ mut}$;*qrf* strains that allow the expression of *qrf* in *trans*. The *frq*$^{qLRE\ mut}$ construct is at the *his-3* locus, and *qrf* is expressed only from the *csr-1* locus. The red dashed line indicates that the *frq* promoter region is deleted in the *qrf* construct to abolish *frq* expression. (b) Strand-specific RT-qPCR results showing that only *qrf* is expressed from the *qrf* construct in the *frq*^{10}; qrf strain. (c) *qrf* expression does not repress *frq* transcription in *trans*. Strand-specific RT-qPCR results showing the levels of *frq* and *qrf* transcripts in the indicated strains in LL. Error bars are standard deviations. Asterisk indicates P value < 0.05 (n=3). (d) Northern blot results showing that expression of *qrf* in *trans* in the *frq*^{10};*frq*$^{qLRE\ mut}$;*qrf* strains does not repress *frq* expression. Densitometric analysis of the northern blot results is shown at right. (e-f) WC ChIP assays showing the relative WC binding levels at the *frq* promoter in LL in the indicated strains. The *wc* double mutant (*wcc*^{DKO}) was used as a negative control for ChIP. n.s. indicates the lack of statistically significance (n=3). (g) Strand-specific RT-qPCR results showing that the mutation of the qLRE element in the *qrf* promoter results in significant increases in light-induced *frq* pre-mRNA expression. (h) Northern blot results showing that the stability of *frq* mRNA is not affected by the transcription of *qrf*. The *frq*^{10};frq.aq strain that can induce *qrf* expression in the presence of QA was used. Thiolutin, a transcription

inhibitor[30], was added in the culture to block *frq* transcription so that *frq* mRNA stability could be determined. Cultures were harvested at the indicated time points after the addition of thiolutin.

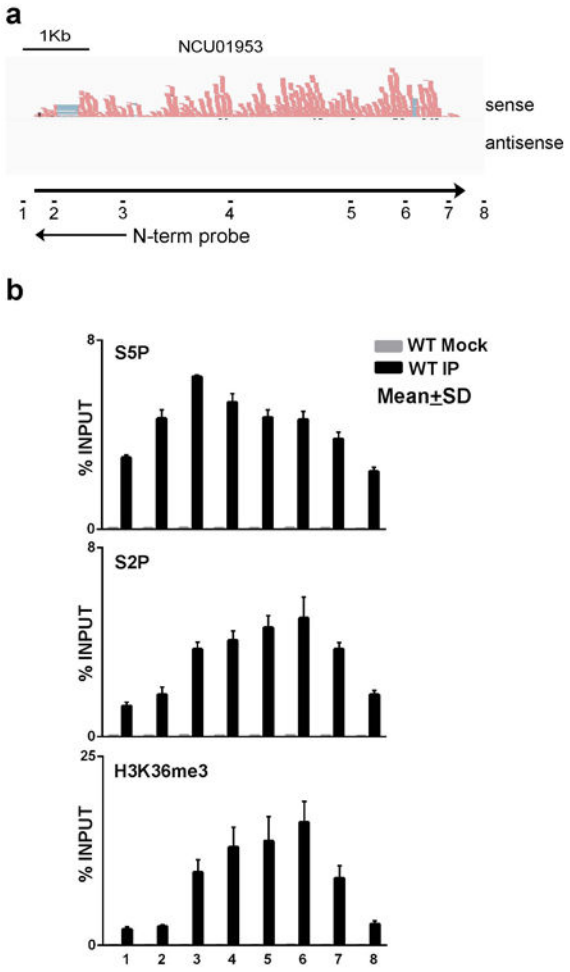

Extended Data Figure 7.

(a) The top panel showing the strand-specific RNA-Seq results of the NCU01953 locus. The bottom panel showing the primers positions used for ChIP assays and riboprobe position used for Northern blot analysis. (b) The ChIP assays showing the relative enrichment of Pol II Ser5 phosphorylation, Pol II Ser2 phosphorylation, and H3K36me3 at the NCU01953 locus in the wild-type strain. Scale on y axis is the enrichment percentage of immunoprecipitation (IP) over input. IgG was used as the mock control for IP.

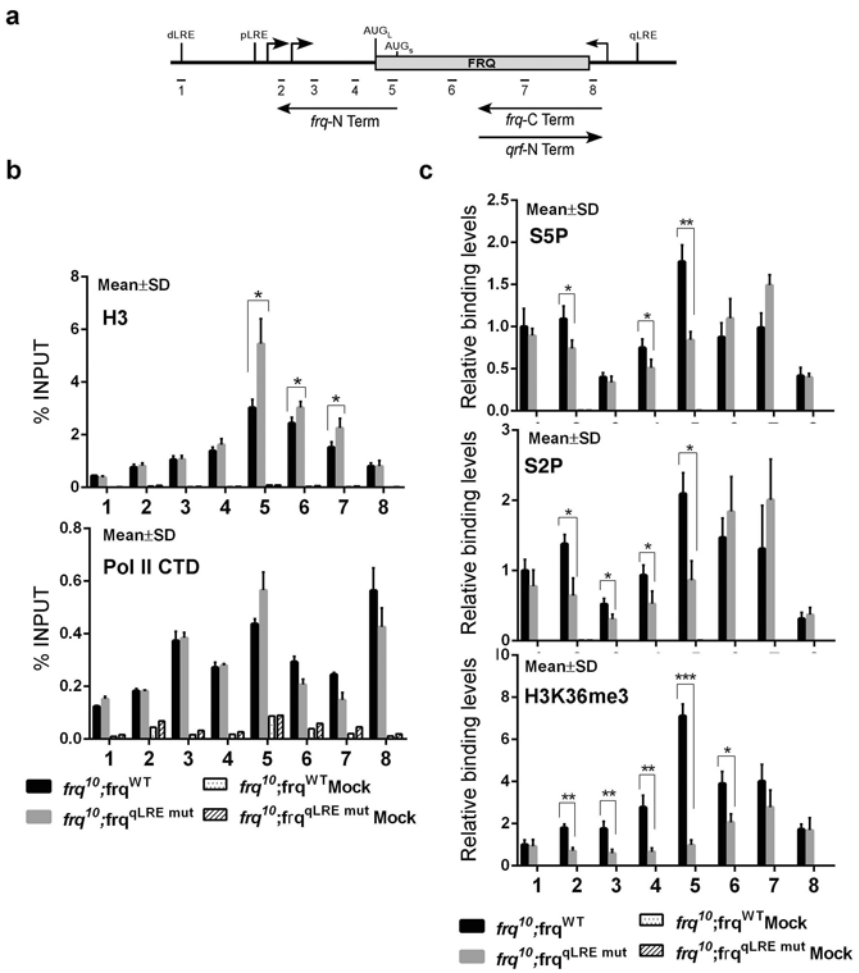

Extended Data Figure 8.

(a) A diagram showing the primers positions at the *frq* locus used for ChIP assays and riboprobes positions used for Northern blot analyses. (b) The ChIP assays showing the relative enrichment of histone H3 and Pol II CTD in the *frq* locus. Scale on y axis is the enrichment percentage of immunoprecipitation (IP) over input. IgG was used as the mock control for IP. (c) The ChIP assays showing the relative enrichment of Pol II Ser5 phosphorylation and Pol II Ser2 phosphorylation (ChIP data in Figure 4b normalized by Pol II CTD ChIP results in panel b), and H3K36me3 (ChIP data in Figure 4b normalized by Histone H3 ChIP results in panel b). Asterisks indicate differences that are statistically significant (*P<0.05, **P<0.01, ***P<0.001).

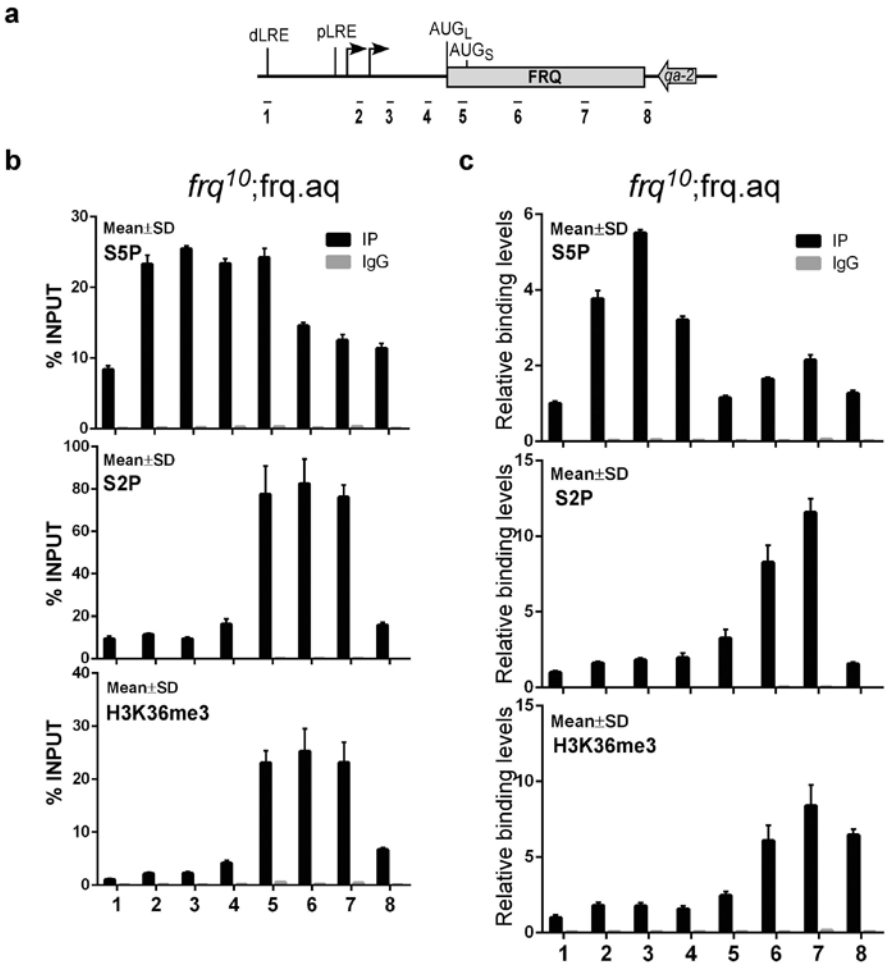

Extended Data Figure 9.

Complete abolishment of *qrf* expression changes the distributions of phosphorylated pol II CTD to a normal profile. (a) A diagram showing the primers positions used for ChIP assays. (b) The ChIP assays showing the relative enrichment of Pol II Ser5 phosphorylation, Pol II Ser2 phosphorylation, and H3K36me3 in the *frq* locus in the *frq*^{10};frq.aq strain in medium with 2% glucose. Under such a condition, qrf expression is completely abolished (shown in Figure 2a). (c) The ChIP assays showing the relative enrichment of Pol II Ser5 phosphorylation and Pol II Ser2 phosphorylation (ChIP data in panel b were normalized by Pol II CTD ChIP results), and H3K36me3 (ChIP data in panel b were normalized by Histone H3 ChIP results).

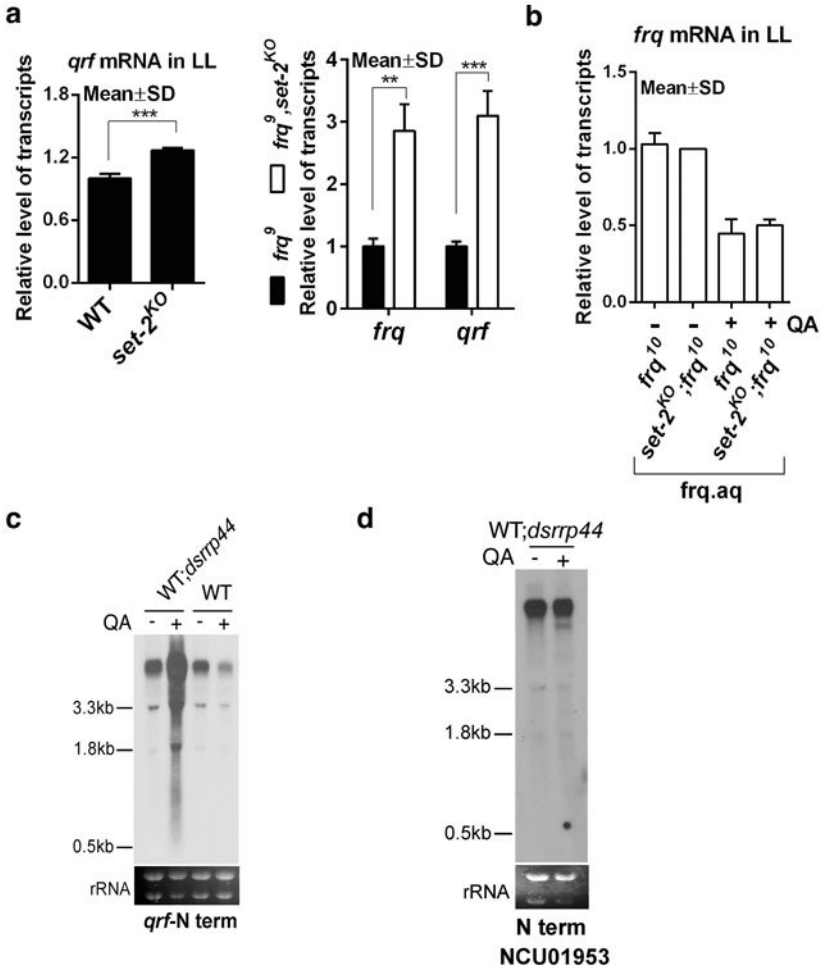

Extended Data Figure 10.

(a) The densitometric analyses of three independent experiments shown in Figure 4c are shown. (b) The densitometric analyses of independent experiments shown in Figure 4d are shown. (c) Northern blot analysis using a N-term probe (marked in Extended Data Figure 8a) specific for the 5′half of *qrf* transcripts in the WT and WT;*dsrrp44* strains in LL. (d) Northern blot analysis using a N-term probe (marked in Extended Data Figure 7a) specific for the 5′half of NCU01953 transcripts in the WT;*dsrrp44* strain in LL.

Acknowledgments

We thank Joonseok Cha, Yunkun Dang and Haiyan Yuan for technical assistance and Dr. Bing Li for critical comments. Supported by grants from the National Institutes of Health to Y.L. (GM068496, GM062591) and N.L.G. (GM081597), the Welch Foundation (I-1560) to Y.L. and BBSRC (BBS/S/C2005/13012) to S.A. and S.K.C.

References

1. Dunlap JC. Molecular bases for circadian clocks. Cell. 1999; 96:271–290. [PubMed: 9988221]
2. Berretta J, Morillon A. Pervasive transcription constitutes a new level of eukaryotic genome regulation. EMBO Rep. 2009; 10:973–982. [PubMed: 19680288]
3. Kramer C, Loros JJ, Dunlap JC, Crosthwaite SK. Role for antisense RNA in regulating circadian clock function in Neurospora crassa. Nature. 2003; 421:948–952. [PubMed: 12607002]

4. Nagano T, et al. The Air noncoding RNA epigenetically silences transcription by targeting G9a to chromatin. Science. 2008; 322:1717–1720. [PubMed: 18988810]
5. Deuve JL, Avner P. The coupling of X-chromosome inactivation to pluripotency. Annu Rev Cell Dev Biol. 2011; 27:611–629. [PubMed: 21801017]
6. Camblong J, Iglesias N, Fickentscher C, Dieppois G, Stutz F. Antisense RNA stabilization induces transcriptional gene silencing via histone deacetylation in S. cerevisiae. Cell. 2007; 131:706–717. [PubMed: 18022365]
7. Ogawa Y, Sun BK, Lee JT. Intersection of the RNA interference and X-inactivation pathways. Science. 2008; 320:1336–1341. [PubMed: 18535243]
8. Prescott EM, Proudfoot NJ. Transcriptional collision between convergent genes in budding yeast. Proc Natl Acad Sci U S A. 2002; 99:8796–8801. [PubMed: 12077310]
9. Hobson DJ, Wei W, Steinmetz LM, Svejstrup JQ. RNA polymerase II collision interrupts convergent transcription. Mol Cell. 2012; 48:365–374. [PubMed: 23041286]
10. Heintzen C, Liu Y. The Neurospora crassa circadian clock. Adv Genet. 2007; 58:25–66. [PubMed: 17452245]
11. Crosthwaite SK, Dunlap JC, Loros JJ. *Neurospora wc-1* and *wc-2*: Transcription, photoresponses, and the origins of circadian rhythmicity. Science. 1997; 276:763–769. [PubMed: 9115195]
12. He Q, et al. White collar-1, a DNA binding transcription factor and a light sensor. Science. 2002; 297:840–843. [PubMed: 12098705]
13. Froehlich AC, Liu Y, Loros JJ, Dunlap JC. White Collar-1, a circadian blue light photoreceptor, binding to the frequency promoter. Science. 2002; 297:815–819. [PubMed: 12098706]
14. Smith KM, et al. Transcription factors in light and circadian clock signaling networks revealed by genomewide mapping of direct targets for neurospora white collar complex. Eukaryot Cell. 2010; 9:1549–1556. [PubMed: 20675579]
15. Aronson BD, Johnson KA, Dunlap JC. The circadian clock locus *frequency*: A single ORF defines period length and temperature compensation. Proceedings of the National Academy of Sciences, USA. 1994; 91:7683–7687.
16. Gooch VD, et al. Fully codon-optimized luciferase uncovers novel temperature characteristics of the Neurospora clock. Eukaryot Cell. 2008; 7:28–37. [PubMed: 17766461]
17. Bell-Pedersen D, Dunlap JC, Loros JJ. Distinct cis-acting elements mediate clock, light, and developmental regulation of the *Neurospora crassa eas* (*ccg-2*) gene. Molecular and Cellular Biology. 1996; 16:513–521. [PubMed: 8552078]
18. Hong CI, Jolma IW, Loros JJ, Dunlap JC, Ruoff P. Simulating dark expressions and interactions of frq and wc-1 in the Neurospora circadian clock. Biophys J. 2008; 94:1221–1232. [PubMed: 17965132]
19. Chang SS, Zhang Z, Liu Y. RNA interference pathways in fungi: mechanisms and functions. Annu Rev Microbiol. 2012; 66:305–323. [PubMed: 22746336]
20. Dang Y, Li L, Guo W, Xue Z, Liu Y. Convergent Transcription Induces Dynamic DNA Methylation at disiRNA Loci. PLoS Genet. 2013; 9:e1003761. [PubMed: 24039604]
21. Belden WJ, Lewis ZA, Selker EU, Loros JJ, Dunlap JC. CHD1 remodels chromatin and influences transient DNA methylation at the clock gene frequency. PLoS Genet. 2011; 7:e1002166. [PubMed: 21811413]
22. Hsin JP, Manley JL. The RNA polymerase II CTD coordinates transcription and RNA processing. Genes Dev. 2012; 26:2119–2137. [PubMed: 23028141]
23. Li B, Howe L, Anderson S, Yates JR, Workman JL. The Set2 histone methyltransferase functions through the phosphorylated carboxyl-terminal domain of RNA polymerase II. J Biol Chem (3rd). 2003; 278:8897–8903. [PubMed: 12511561]
24. Adhvaryu KK, Morris SA, Strahl BD, Selker EU. Methylation of histone H3 lysine 36 is required for normal development in Neurospora crassa. Eukaryot Cell. 2005; 4:1455–1464. [PubMed: 16087750]
25. Zhou Z, et al. Suppression of WC-independent frequency transcription by RCO-1 is essential for Neurospora circadian clock. Proc Natl Acad Sci U S A. 2013; 110:E4867–4874. [PubMed: 24277852]

26. Guo J, Cheng P, Yuan H, Liu Y. The exosome regulates circadian gene expression in a posttranscriptional negative feedback loop. Cell. 2009; 138:1236–1246. [PubMed: 19747717]
27. Sauman I, Reppert SM. Circadian clock neurons in the silkmoth Antheraea pernyi: novel mechanisms of Period protein regulation. Neuron. 1996; 17:889–900. [PubMed: 8938121]
28. Koike N, et al. Transcriptional architecture and chromatin landscape of the core circadian clock in mammals. Science. 2012; 338:349–354. [PubMed: 22936566]
29. Menet JS, Rodriguez J, Abruzzi KC, Rosbash M. Nascent-Seq reveals novel features of mouse circadian transcriptional regulation. Elife. 2012; 1:e00011. [PubMed: 23150795]
30. Vollmers C, et al. Circadian oscillations of protein-coding and regulatory RNAs in a highly dynamic mammalian liver epigenome. Cell Metab. 2012; 16:833–845. [PubMed: 23217262]
31. Choudhary S, et al. A double-stranded-RNA response program important for RNA interference efficiency. Mol Cell Biol. 2007; 27:3995–4005. [PubMed: 17371837]
32. Zhao Y, et al. Ubiquitin ligase components Cullin4 and DDB1 are essential for DNA methylation in Neurospora crassa. J Biol Chem. 2010; 285:4355–4365. [PubMed: 19948733]
33. Bardiya N, Shiu PK. Cyclosporin A-resistance based gene placement system for Neurospora crassa. Fungal genetics and biology : FG & B. 2007; 44:307–314. [PubMed: 17320431]
34. Liu Y, Garceau N, Loros JJ, Dunlap JC. Thermally regulated translational control mediates an aspect of temperature compensation in the *Neurospora* circadian clock. Cell. 1997; 89:477–486. [PubMed: 9150147]
35. Dharmananda, S. Studies of the Circadian Clock of Neurospora crassa: Light-induced Phase Shifting. University of California; Santa Cruz: 1980.
36. Barlow JJ, Mathias AP, Williamson R, Gammack DB. A Simple Method for the Quantitative Isolation of Undegraded High Molecular Weight Ribonucleic Acid. Biochem Biophys Res Commun. 1963; 13:61–66. [PubMed: 14069514]
37. Yoon OK, Brem RB. Noncanonical transcript forms in yeast and their regulation during environmental stress. RNA. 2010; 16:1256–1267. [PubMed: 20421314]
38. He Q, Liu Y. Molecular mechanism of light responses in Neurospora: from light-induced transcription to photoadaptation. Genes & Dev. 2005; 19:2888–2899. [PubMed: 16287715]
39. Pall ML. The use of Ignite (Basta; glufosinate;phosphinothricin) to select transformants of bar-containing plasmids in *Neurospora crassa*. Fungal Genetics Newsletter. 1993; 40
40. Ruoff P, Loros JJ, Dunlap JC. The relationship between FRQ-protein stability and temperature compensation in the *Neurospora* circadian clock. Proc Natl Acad Sci USA. 2005; 102:17681–17686. [PubMed: 16314576]
41. Ruoff P, Vinsjevik M, Monnerjahn C, Rensing L. The Goodwin oscillator: on the importance of degradation reactions in the circadian clock. J Biol Rhythms. 1999; 14:469–479. [PubMed: 10643743]
42. Yu Y, et al. A genetic network for the clock of Neurospora crassa. Proc Natl Acad Sci U S A. 2007; 104:2809–2814. [PubMed: 17301235]
43. Gear C. Simultaneous Numerical Solution of Differential-Algebraic Equations. IEEE Transactions on Circuits and Systems. 1971; 18:89–95.
44. Ermentrout B. XPPAUT. Scholarpedia. 2007; 2:1399.

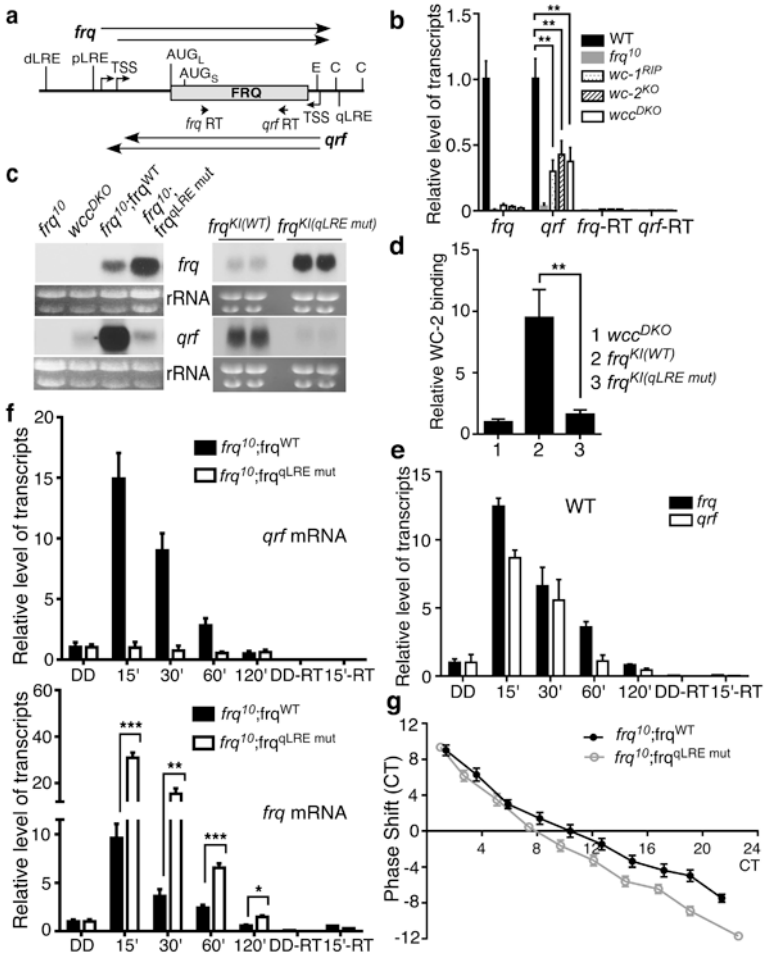

Figure 1.

WC-mediated light-induction of *qrf* represses *frq* to regulate light resetting of the clock. (a) A diagram showing the *frq* locus. E: *Eco*R V site. C: *Cla* I site. (b) Strand-specific RT-qPCR analyses showing the levels of *frq* and *qrf* in LL. *frq*-RT and q*rf*-RT are control reactions without reverse transcriptase. Error bars are SD (n=3). (c) Northern blot analyses showing the expression of *frq* and *qrf* in LL. (d) WC-2 ChIP assays showing the WC binding levels at the qLRE of *qrf* promoter in LL. (e-f) Strand-specific qRT-PCR analyses showing the levels of *frq* and *qrf* after a 2 min of light induction at DD24. (g) Phase response curves of conidiation rhythms after 2 min of light pulse at different circadian time points. *P<0.05, **P<0.01, ***P<0.001.

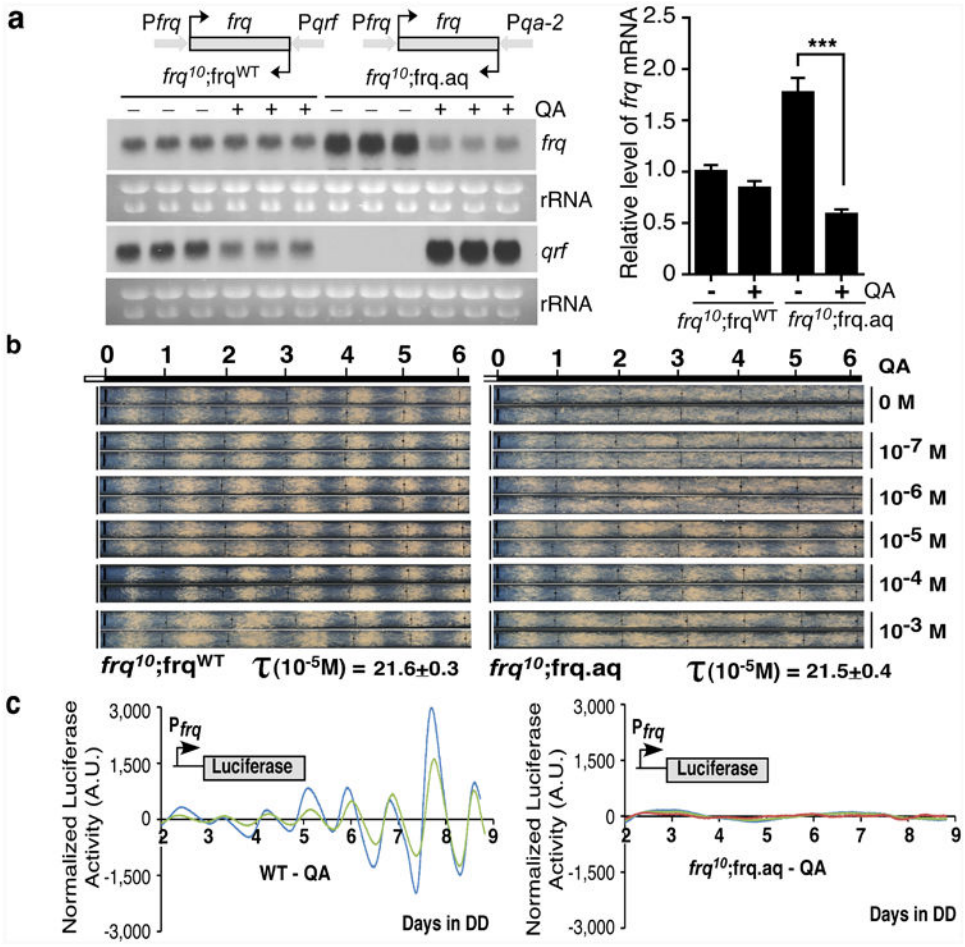

Figure 2.

qrf expression is required for circadian rhythmicities. (a) Northern blot analysis showing the levels of *frq* and *qrf* with/without 1×10^{-3} M QA (0.1% glucose) in LL. Right panel shows the densitometric analyses of the results. Error bars are SD. (b) Race tube analyses of the indicated strains (0.1% glucose with different concentrations of QA) in DD. (c) Luciferase reporter assay showing the normalized *frq* promoter activity after two days in DD.

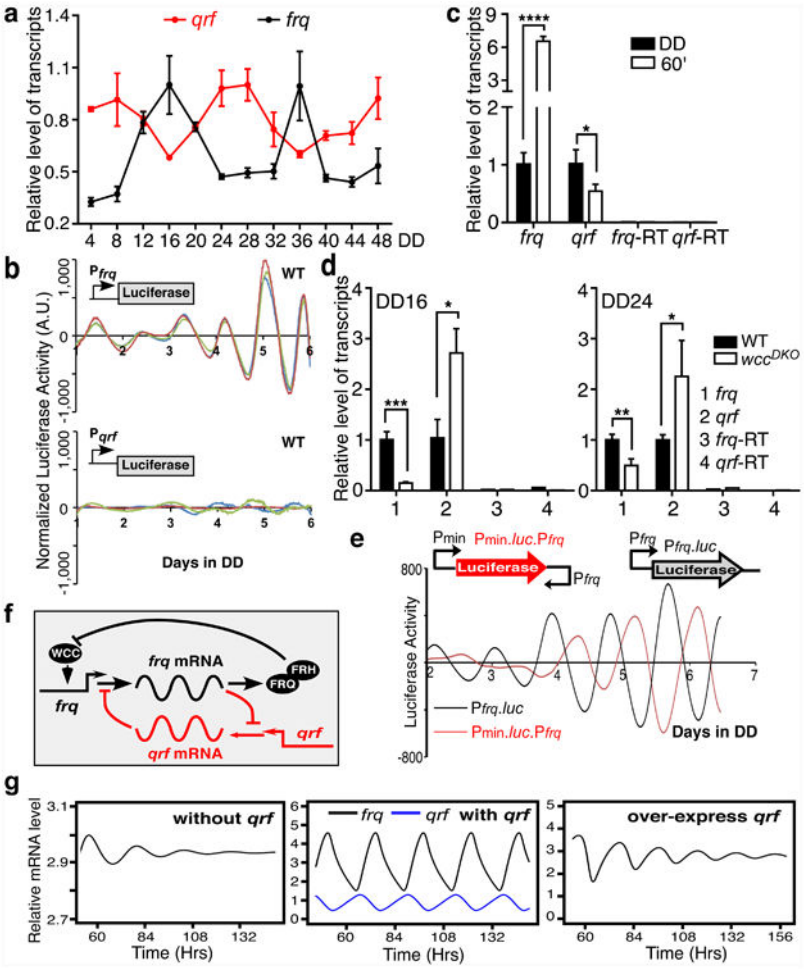

Figure 3.

Mutual inhibition of *frq* and *qrf* transcription forms a double negative feedback loop that is required for clock function. (a) Strand-specific RT-qPCR results showing the oscillations of *frq* and *qrf* in DD. Error bars are SD (n=3). (b) Luciferase reporter assay showing the normalized *frq* or *qrf* promoter activity after one day in DD in wild-type strains with the Pfrq:luc or Pqrf:luc construct. (c) Strand-specific RT-qPCR results showing the levels of *frq* and *qrf* in the frq^{10};$frq^{qLRE\ mut}$ strain at DD24 or 60 min after the dark to light transfer. (d) Levels of *frq* and *qrf* in the wild-type and wcc^{DKO} strains measured by strand-specific RT-qPCR in DD. (e) Luciferase reporter assays showing the normalized luminescence levels in a wild-type strain that carries the Pfrq.*luc* (black) or Pmini.*luc*.Pfrq (red) construct. (f) A model of the *Neurospora* oscillator. (g) Mathematical simulation of relative *frq* levels in DD without *qrf* (k19 =0) (left), with *qrf* (k16=0.5, k17=0.35, k19=0.1) (middle), and with *qrf* over-expression (k16 =0.91) (right).

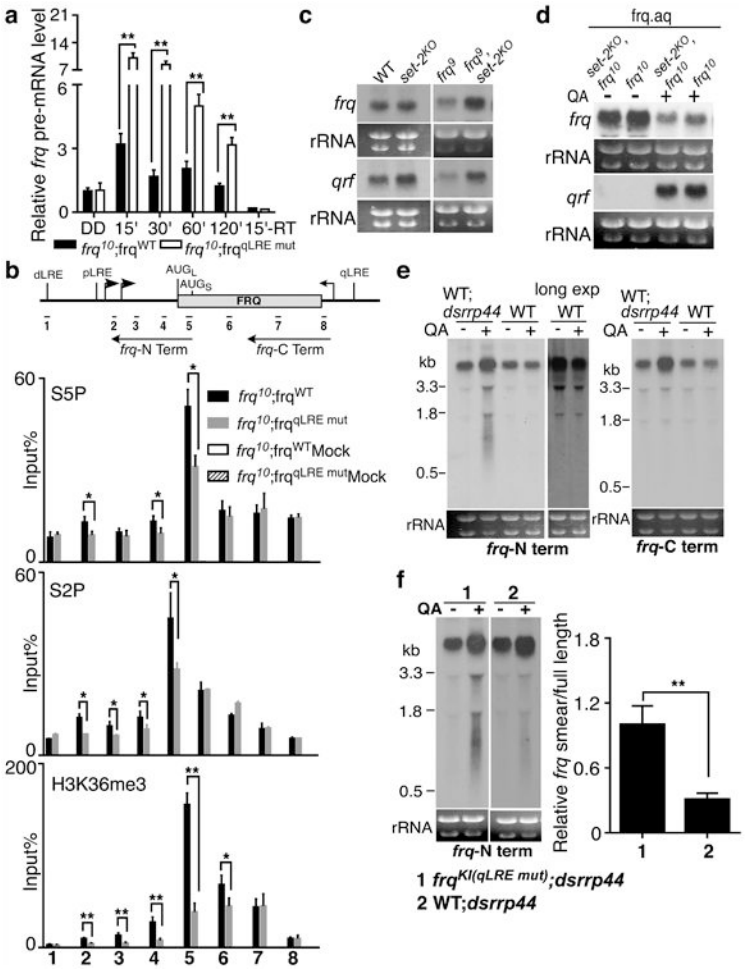

Figure 4.

qrf transcription results in pol II stalling, premature transcription termination and chromatin modifications. (a) Strand-specific RT-qPCR results showing the levels of intron-containing *frq* after dark to light transfer. (b) ChIP assays showing the relative enrichment of pol II Ser 5, Ser 2, and H3K36me3 in the *frq* locus in LL. IgG was used as the mock control for IP. (c-d) Northern blot analyses showing the levels of *frq* and *qrf* in LL. (e-f) Northern blot analysis in LL. *frq*-N term and *frq*-C term are specific for the 5′ or 3′ half of the *frq* transcripts, respectively (shown in Figure 4b). The addition of QA results in *rrp44* silencing. The ratios between truncated and full-length *frq* transcripts from three independent experiments in (f) are shown. Error bars are SD. *P<0.05, **P<0.01.